

SAMAY S24: a novel wireless ‘online’ device for real-time monitoring and analysis of volumetric capnography

M. Vallarino¹, L. Quintela¹, G. Jorge¹, G. Lorenzo¹, C. Nan², M. Ispert¹, J.P. Bouchacourt¹, J.C. Grignola¹

¹Facultad de Medicina, Hospital de Clínicas; ²Facultad de Veterinaria.

Universidad de la República, Montevideo, Uruguay.

Abstract—Volumetric capnography (VCap) provides information about CO₂ exhaled per breath (VCO₂br) and physiologic dead space (VDphys). A novel wireless device with a high response time CO₂ mainstream sensor coupled with a digital flowmeter was designed to monitor all VCap parameters online in rabbits (SAMAY S24).

Ten New Zealand rabbits were anesthetized and mechanically ventilated. VCO₂br corresponds to the area under the VCap curve. We used the modified Langley method to assess the airway VD (VDaw) and the alveolar CO₂ pressure. VDphys was estimated using Bohr’s formula, and the alveolar VD was calculated by subtracting VDaw from VDphys. We compared (Bland-Altman) the critical VCap parameters obtained by SAMAY S24 (Langley) with the Functional Approximation based on the Levenberg-Marquardt Algorithm (FA-LMA) approach during closed and opened chest conditions.

SAMAY S24 could assess dead space volumes and VCap shape in real time with similar accuracy and precision compared to the ‘offline’ FA-LMA approach. The opened chest condition impaired CO₂ kinetics, decreasing the phase II slope, which was correlated with the volume of CO₂ exhaled per minute.

Keywords—volumetric capnography, physiological dead space, airway dead space, alveolar dead space, Enghoff index.

I. INTRODUCTION

Capnography provides a noninvasive, continuous display of the fractional concentration or partial pressure of CO₂ in breathing gases during the respiratory cycle [1]. The capnogram may be recorded by mainstream or sidestream techniques and against time (Time-based capnography or time capnography -TCap-) or the expired tidal volume (Volume-based or volumetric capnography -VCap-). Sidestream capnography led to a dynamic distortion of the CO₂ concentration curve (transit time) compared with the mainstream approach regarded as a reference technique [2]. Time- and volume-based graphical presentations have a similar appearance and can be used to monitor the end-tidal pressure of CO₂ (PETCO₂). Only VCap provides information about the volume of physiologic (VDphys), airway (VDaw), and alveolar dead space (VDalv); the volume of CO₂ exhaled per breath (VCO₂br) and minute (VCO₂) [3][4]. Two critical aspects shared by all methods of VCap analysis are the accurate measurement of the alveolar PCO₂ (PACO₂), which is critical in estimating the VDphys (Bohr’s formula), and the accurate determination of the location of the “airway-alveolar” interface (the limit between VDaw and alveolar tidal volume, VTalv) which allows for estimating the VDalv. Although modern mechanical ventilators have incorporated a

VCap module, it displays limited VCap parameters ‘online’, and the internal software is generally unknown. Tusman et al. have proposed a Functional Approximation of the VCap (NICO mainstream capnography, Respironics, Wallingford, CT, USA) based on a Levenberg-Marquardt Algorithm (FA-LMA) using a custom-made MATLAB program (MathWorks, Natick, MA). They showed less bias and dispersion for calculating VDaw ‘offline’ compared to the traditional Fowler’s method beyond the VCap shape [5]. They also validated the estimation of PACO₂ as the midpoint of the slope of phase III, applying the mathematical algorithm of the multiple inert gas elimination technique (MIGET) [6].

We present a novel wireless (Wi-Fi) capnograph device for real-time monitoring of a complete set of VCap parameters through a robust own-developed software without any fitting model to customize VCap shape. The purposes of this study were: 1) to provide a novel wireless ‘online’ device for real-time monitoring and analysis of VCap; 2) to use a modified Langley method to get VDaw and PACO₂; 3) to compare the modified Langley method with FA-LMA approach in anesthetized and mechanically ventilated rabbits.

II. METHODOLOGY

Ten adult female New Zealand rabbits (3.0±0.5 kg) were anesthetized (midazolam 0.5-1 mg/kg/h, fentanyl 5 µg/kg/h) and rocuronium 0.6 mg/kg/h), tracheotomized and mechanically ventilated via a cuffed endotracheal tube. The ventilator was set in the volume-controlled ventilation mode with a VT of ~7 mL/kg, end-expiratory pressure of 5 cmH₂O, a respiratory rate of 28±6 breaths/min (ensuring PaCO₂ ~40 mmHg and pH 7.35-7.44) and inspired fractional oxygen of 60%. Systemic arterial oxygen saturation was monitored and maintained above 96% (Rainbow 7 LNOP newborn sensor, Radical 7, Masimo Corporation, Irvine, CA, USA). We placed a fluid-filled catheter (20-gauge) in the left jugular vein and the right femoral artery to measure central venous pressure (CVP) and aortic blood pressure (AoP), respectively. The arterial partial pressure of oxygen and CO₂ were monitored by serial blood gas evaluation (ABL520, Radiometer, Denmark). We used a heating pad to keep the animal normothermia.

This study was approved by the Ethics Committee on the Use of Animals (CEUA), Facultad de Medicina, Universidad de la República, Montevideo-Uruguay in October 2019 (Ethical Committee N° 070153-000141-19). We strictly complied with the Guide for the Care and Use of Laboratory

Animals (NIH Publication N° 85-23, revised 1996), prepared by the National Academy of Sciences' Institute for Laboratory Animal Research.

A. Data acquisition and analysis

CO₂ is measured by a CO₂ mainstream, non-dispersive infrared sensor (response time ~10 msec, accuracy of ±0.2%, and resolution 0.1%) (QuRe, Treaton) clipped onto a neonatal/pediatric digital flowmeter (dead space <1 mL, accuracy of ±0.02 L/min, and resolution 5 mL/min) (SFM3400-AW, Sensirion) with a time delay about 2.5 msec (Fig.1.Top). Airway pressure (AwP) was measured by a digital pressure transducer (Honeywell HSC series). The three signals were recorded continuously with a sample rate of 200Hz by linear interpolation using a developed hardware and software wireless (Wi-Fi) connection with a laptop, tablet, or mobile phone by a web browser (SAMAY S24, SAMAY Instruments, Montevideo-URUGUAY). The device can support up to four monitors simultaneously with a storage capacity of 1536 hours of registration. Temporal airflow and the integration of the corresponding volume (compensated for body temperature and saturated water vapor pressure -BTSPS-), TCap, and AwP were displayed in real-time together with the AwP-Volume and exhaled PCO₂-Volumen (VCap) loops. The device's high resolution lets us simultaneously display instantaneous calculated values for each respiratory cycle of VT (inspiratory -VCI- and expiratory -VCE- VT), peak AwP (Pmax), positive end-expiratory pressure (PEEP), respiratory frequency (FR), inspiratory (Ti) and expiratory (Te) times, and Ti:Te ratio, PETCO₂, mean alveolar partial pressure of CO₂ (PACO₂), mean expiratory partial pressure of CO₂ (PECO₂), VDphys (VDb/VT), VDaw, and VDalv. Finally, VCO₂ and VCap slopes of phase II (SV-II) and phase III (SV-III) were obtained by the moving average of ten respiratory cycles (Fig.1. Bottom).

The VCap presents three phases corresponding to the sequential compartments from which the expired CO₂ comes. Phase I (VI) corresponds to the first part of the exhaled volume free of CO₂. Phase II (VII) corresponds to a transition phase with a rapid rise in expired CO₂ corresponding to proximal alveolar-capillary units and rapid emptying (with low time constants). Phase III (VIII) represents pure alveolar gas and corresponds to expired CO₂ from distal alveolar-capillary units and slow emptying (with high time constants). All three phases were calculated offline by FA-LMA approach and expressed as VT ratios (Fig.2) [5].

PETCO₂ and PECO₂ were calculated as the last expiratory CO₂ value immediately before the start of the next inspiration and by multiplying the expired fraction of CO₂ by the dry barometric pressure, respectively. VDaw was estimated by the volume intercept of a linear regression performed on the expiratory CO₂ volume versus exhaled volume plot (Langley method). We discarded the first 20% ascending part of the expired CO₂ to exclude the curvilinear part of the volumetric capnogram corresponding to phase II. PACO₂ was determined at the midpoint of phase III, defined at 55% of the expired CO₂ [7] [8]. The VDphys was obtained using Bohr's original formula:

$$VD_{phys} \text{ (Bohr)} = \frac{(PACO_2 - PECO_2)}{PACO_2}$$

VD_{alv} was calculated by subtracting VD_{aw} from VD_{phys} [8]. VCO₂ was obtained by the product of VCO₂br (which corresponds to the area under the VCap curve) and respiratory frequency.

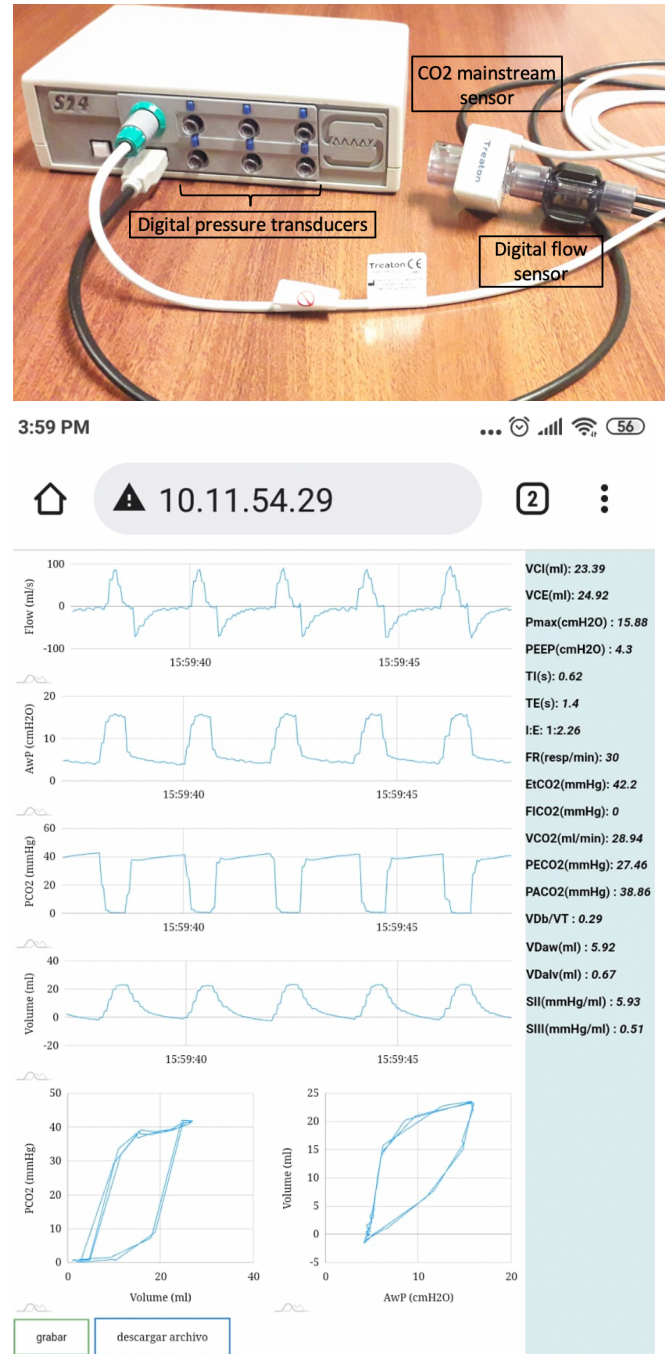


Fig.1. **Top:** SAMAY S24. **Bottom:** Online temporal signals and calculated variables monitored by S24 on an android mobile phone screen.

SV-II and SV-III were determined by fitting a linear regression line (least squares method) between ±20% of VD_{aw} and ±20% of the VCO₂ corresponding to the PACO₂, respectively. A coefficient of r ≥ 0.9 was accepted (Fig.2).

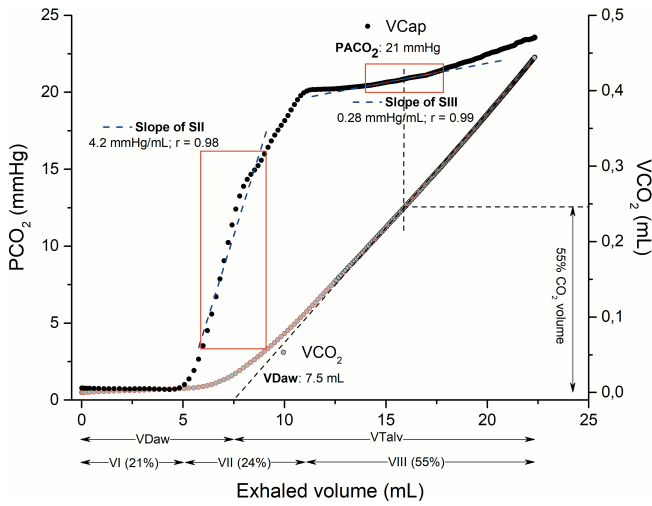


Fig.2. A representative opened chest volumetric capnogram (VCap, black circles) and the exhaled CO₂ volume versus exhaled tidal volume plot (grey circles) showing how the S24 software works. VDaw is determined by the volume intercept of a linear regression performed on the exhaled CO₂ volume versus exhaled volume plot (dotted line), and PACO₂ is estimated by the midpoint of phase III defined at 55% of the exhaled CO₂ volume (modified Langley method) [7]. The red rectangles define the range of points used for fitting the linear regression line of SV-II and SV-III slopes.

We estimated Enghoff's index (VDEng) as an index of global inefficiency of gas exchange replacing PACO₂ by the arterial partial pressure of CO₂ (PaCO₂) in Bohr's formula. VDEng adds the fiducial dead space, including the shunting and low V/Q regions of the lungs (venous admixture):

$$VDEng = \frac{(PaCO_2 - PECO_2)}{PaCO_2}$$

We also estimated the equivalent of CO₂ by minute ventilation/VCO₂ (MV/VCO₂). SV-II and SV-III were normalized by the corresponding PECO₂ (SnV-II, mL⁻¹, and SnV-III, mL⁻¹), what allowed the comparison of slopes from breaths with different CO₂ excretion rates and VT of different sizes [9] [10]. Online data were stored on a laptop using an exportable excel template to complete offline calculations. Whole CO₂ kinetics was analyzed under closed (CC) and opened chest (OC) conditions.

SV-II and SV-III were correlated with VCO₂. VDaw and PACO₂ assessment by the FA-LMA approach and the modified Langley method were compared by correlation analysis and Bland-Altman agreement analysis by calculating the bias (mean of the difference between two methods) and the 95% limits of agreement (1.96 standard deviations around the mean difference). P-value <0.05 was considered statistically significant (SPSS version 21.0.).

III. RESULTS

Table 1 shows data for dead space volumes and fractions, CO₂ kinetics, and shape-related capnography parameters during both experimental conditions. All dead spaces did not change beyond the experimental condition. However, VDEng was significantly higher than VDphys (Bohr) in both

experimental conditions, associated with a high Pa-PACO₂ gradient (14±3 and 12±4 mmHg, respectively).

The assessment of VDaw and PACO₂ showed a significant correlation between the modified Langley method and FA-LMA approach during both experimental conditions. The Bland-Altman analysis showed a negligible bias between the two methodologies for VDaw and PACO₂ estimations, and the 95% limits of agreement with FA-LMA approach were <2% (Table 2).

Opened chest condition determined a significant decrease (~11-14%) of PETCO₂, PACO₂, PECO₂, and VCO₂ despite a similar MV. Therefore, the equivalent of CO₂ was significantly impaired. The proportion of the VCap phases and the airway-alveolar interface (inflection point of SII slope) did not show significant changes (Table 1). Only the SV-II slope decreased (P <0.05) and correlated with VCO₂ (r = 0.66; P =0.012). However, the SV-II and SV-III slopes normalized by exhaled CO₂ (PECO₂) did not show significant differences.

TABLE 1. CAPNOGRAPHY VALUES

	Closed Chest, CC	Opened Chest, OC
VT, mL	20±2	21±2
VDphys, mL	7.1±0.7	7.3±0.6
VDaw, mL	6.3±0.6	6.6±0.6
VDalv, mL	0.7±0.1	0.8±0.2
VDaw/VT, %	36±10	37±10
VDphys (Bohr)	0.36±0.02	0.35±0.02
VDEng	0.59±0.06#	0.58±0.09#
PetCO ₂ , mmHg	31±5	27±4*
PACO ₂ , mmHg	29±5	25±5*
PECO ₂ , mmHg	18±3	16±3*
VCO ₂ , mL/min	16.4±2.3	14.6±2.7*
VCO ₂ br/VT	0.028±0.004	0.024±0.003*
MV, mL/min	578±42	608±53
MV/VCO ₂	36±5	42±6*
SV-II, mmHg/mL	5.5±0.7	4.7±0.7*
SnV-II, mL ⁻¹	0.30±0.03	0.29±0.03
SV-III, mmHg/mL	0.38±0.10	0.36±0.12
SnV-III, mL ⁻¹	0.02±0.006	0.02±0.009
VI/VT, %	22±3	21±3
VII/VT, %	26±4	25±4
VIII/VT, %	51±3	54±4

Data are mean±SD; n = 10; *p<0.05 vs. Closed chest; #p<0.05 vs. VDBohr in each experimental condition (Wilcoxon signed-rank test).

TABLE 2. LINEAR REGRESSION AND BLAND-ALTMAN ANALYSIS FOR VDaw AND PACO₂ ESTIMATION OBTAINED WITH FA-LMA APPROACH AND MODIFIED LANGLEY METHOD

Variables	Regression		Bland-Altman	
	Slope	R ²	Bias	1.96 SD
VDaw, mL (CC)	1.05	0.95	0.12 (1.8%)	0.28
VDaw, mL (OC)	0.87	0.80	0.01 (0.1%)	0.66
PACO ₂ , mmHg (CC)	0.99	0.99	-0.36 (1.3%)	0.46
PACO ₂ , mmHg (OC)	0.97	0.99	-0.34 (1.4%)	0.77

Mean AoP and CVP did not change after opening the chest (57±8 vs. 50±6 mmHg and 4.3±1.6 vs. 4.0±1.5 mmHg, respectively). Neither did the PaCO₂ (43±6 vs. 37±7 mmHg) and arterial pH (7.41±0.03 vs. 7.44±0.07).

IV. DISCUSSION

SAMAY S24 device allowed monitoring of VCap-derived variables, giving complete real-time information about the CO₂ kinetics of mechanically ventilated animals. The high resolution (high response time and sampling rate with a negligible time delay between CO₂ and air flow measurements) enabled to obtain the VDaw and PACO₂ ‘online’ using the modified Langley approach with similar accuracy and precision compared to the ‘offline’ dynamic adaptive FA-LMA approach. In addition, the SV-II and SV-III slopes were obtained ‘online’. In clinical settings, the design of SAMAY S24 would allow the monitoring of patients without needing each patient to be assisted by a mechanical ventilator with a VCap module.

The significant difference between VDphys (Bohr, true dead space) and VDEng would be due to the anesthesia and mechanical ventilation and explain the concomitant high Pa-ACO₂ gradient [10] [11]. The mean values of VDphys (Bohr) and VDEng were similar to the values obtained in children (6.3±5.6 yrs.) mechanically ventilated (0.34±0.12 and 0.42±0.13, respectively) [12].

Closed chest VI/VT, VII/VT, VDaw/VT, SV-II, and SV-III were higher, and VIII/VT was lower than reference values in healthy anesthetized patients (11±4%, 15±4%, 27±6%, 0.036-0.04 mmHg/ml, 0.007-0.017 mmHg/mL, and 75±5%, respectively) [10]. The morphometric of the acinar cross-sectional area could explain this VCap shape difference between rabbits and adult human beings [8]. Something similar occurs between prematurely and term-born infants, where the median (IQR) of SV-II and SV-III of the former were significantly higher compared to the latter ones, respectively (SV-II: 12.4 (10.1-19.5) vs. 6.1 (5.2-7.5); SV-III: 6.1 (5.2-7.5) vs. 0.76 (0.52-1.31) mmHg/mL) [13]. By contrast, VCO₂br/VT values observed were like to healthy subjects (0.028±0.005), which confirms the balance between efficiency of ventilation, distribution of lung perfusion, global V/Q ratio, area of gas exchange, and metabolism [8].

Opened chest impaired CO₂ kinetics, associated with decreased PETCO₂, PACO₂, and VCO₂br/VT without changes in the SV-III, ruling out a significant increase in V/Q inhomogeneity. The lower rise of phase II expired CO₂ (SV-II slope decrease) could correspond to a reduction in the V/Q ratio of the proximal alveolar-capillary units with a higher quantity of CO₂. The associated decrease in PETCO₂, PACO₂, and VCO₂br/VT without changes in the SV-III, ruling out a significant increase in V/Q inhomogeneity. The concomitant fall in the SV-II and PETCO₂ could explain the absence of significant modifications in the VCap phases and the significant correlation between SV-II with VCO₂.

The pulmonary system's resistive and/or elastic properties also affect the shape and various indices derived from the VCap. Csorba et al. showed that in mechanically ventilated patients, the SV-II is linked to the pulmonary elastic recoil [14]. Since the SV-II and SV-III slopes normalized by exhaled CO₂ did not show significant differences, we could consider the absence of significant changes in lung mechanics in the open chest condition.

As a study limitation, the device's software robustness performance was not analyzed for calculating VCap

parameters from severely deformed capnograms by pathological conditions (i.e., acute respiratory distress syndrome).

V. CONCLUSION

We presented a wireless (Wi-Fi) ‘online’ device using a web browser with a high resolution for real-time monitoring a complete set of VCap-derived parameters and supporting up to four digital monitors (tablet, mobile phone, laptop). Although the SAMAY S24 device is compatible with pediatric and adult (Sensirion SFM3300-AW) use, the capnograph's high response time (10 msec), low apparatus dead space (<1 mL), and software sampling rate (200 Hz) should overcome the technical limitations to monitor exhaled CO₂ in newborn patients [15].

ACKNOWLEDGMENT

This work was financed by CSIC (Comisión Sectorial de Investigación Científica); Universidad de la República.

REFERENCES

- [1] P. Kremer, S. H. Böhm, and G. Tusman, “Clinical use of volumetric capnography in mechanically ventilated patients,” *J. Clin. Monit. Comput.*, vol. 34, no. 1, pp. 7–16, 2020.
- [2] A. L. Balogh *et al.*, “Capnogram slope and ventilation dead space parameters: Comparison of mainstream and sidestream techniques,” *Br. J. Anaesth.*, vol. 117, no. 1, pp. 109–117, 2016.
- [3] J. W. Kreit, “Volume capnography in the intensive care unit: Physiological principles, measurements, and calculations,” *Ann. Am. Thorac. Soc.*, vol. 16, no. 3, pp. 291–300, 2019.
- [4] S. Verscheure, P. B. Massion, F. Verschuren, P. Damas, and S. Magder, “Volumetric capnography: Lessons from the past and current clinical applications,” *Crit. Care*, vol. 20, no. 1, pp. 1–9, 2016.
- [5] G. Tusman, A. Scandurra, S. H. Böhm, F. Suarez-Sipmann, and F. Clara, “Model fitting of volumetric capnograms improves calculations of airway dead space and slope of phase III,” *J. Clin. Monit. Comput.*, vol. 23, no. 4, pp. 197–206, 2009.
- [6] G. Tusman, F. S. Sipmann, J. B. Borges, G. Hedenstierna, and S. H. Böhm, “Validation of Bohr dead space measured by volumetric capnography,” *Intensive Care Med.*, vol. 37, no. 5, pp. 870–874, 2011.
- [7] G. Murias, L. Blanch, and U. Lucangelo, “The physiology of ventilation,” *Respir. Care*, vol. 59, no. 11, pp. 1795–1807, 2014.
- [8] R. S. Ream *et al.*, “Volumetric capnography in children,” *Anesthesiology*, vol. 82, pp. 64–73, 1995.
- [9] B. Babik, Z. Csorba, D. Czövek, P. N. Mayr, G. Bogáts, and F. Peták, “Effects of respiratory mechanics on the capnogram phases: importance of dynamic compliance of the respiratory system,” *Crit. Care*, vol. 16, no. 5, 2012.
- [10] G. Tusman *et al.*, “Reference values for volumetric capnography-derived non-invasive parameters in healthy individuals,” *J. Clin. Monit. Comput.*, vol. 27, no. 3, pp. 281–288, 2013.
- [11] G. Tusman, F. S. Sipmann, and S. H. Böhm, “Rationale of dead space measurement by volumetric capnography,” *Anesth. Analg.*, vol. 114, no. 4, pp. 866–874, 2012.
- [12] P. Bourgoin, F. Baudin, D. Brossier, G. Emeriaud, M. Wysocki, and P. Jouvet, “Assessment of bohr and enghoff dead space equations in mechanically ventilated children,” *Respir. Care*, vol. 62, no. 4, pp. 468–474, 2017.
- [13] T. Dassios, P. Dixon, E. Williams, and A. Greenough, “Volumetric capnography slopes in ventilated term and preterm infants,” *Physiol. Meas.*, vol. 41, p. 055001, 2020.
- [14] Z. Csorba *et al.*, “Capnographic Parameters in Ventilated Patients: Correspondence with Airway and Lung Tissue Mechanics,” *Anesth. Analg.*, vol. 122, no. 5, pp. 1412–1420, 2016.
- [15] G. Schmalisch, “Current methodological and technical limitations of time and volumetric capnography in newborns,” *Biomed Eng Online*, vol. 15, no. 104, pp. 1–13, 2016.